Rios, S., C. Ramos, A. Viana da Fonseca, N. Cruz and C. Rodrigues (2017). "Mechanical and durability properties of a soil stabilised with an alkali-activated cement." European Journal of Environmental and Civil Engineering: 1-23.
DOI: 10.1080/19648189.2016.1275987
http://dx.doi.org/10.1080/19648189.2016.1275987

Mechanical and durability properties of a soil stabilized with an alkali-activated cement

Abstract

Alkali activated cements (AAC) have been extensively studied for different applications as an alternative to Portland cement (which has a high carbon footprint) and due to the possibility of including waste materials such fly ash or slags. However, few works have addressed the topic of stabilised soils with AAC for unpaved roads, with curing at ambient temperature, where the resistance to wetting and drying as well as the mechanical properties evolution over time is particularly relevant. In this paper, a silty sand was stabilized with an AAC synthetized from low calcium fly ash and an alkaline solution made from sodium silicate and sodium hydroxide. The evolution of stiffness and strength up to 360 days, the tensile strength, and the performance during wetting and drying cycles were some of the characteristics analysed. Strength and stiffness results show a significant evolution far beyond the 28^{th} curing day, but still with a reasonable short-term strength. Strength parameters deduced from triaxial tests were found to be very high with stress-strain behaviour typical of cemented soils. Durability properties related to resistance to immersion and wetting and drying cycles were found to comply with existing specifications for soil-cement, giving validity for its use as soil-cement replacement.

Keywords: Fly-ash, Alkali-activated cement, Soil improvement, Resistance to Immersion, Curing time, Durability

Introduction

In some countries, low cost roads represent a significant percentage of the road network with an important social and economic impact in the local communities. Being sometimes the fastest link between villages and towns, these roads provide access to basic services like health and education, and enable the transport of agricultural goods to markets and raw materials from forest and mines (Brito, 2011; Fukubayashi and Kimura, 2014). However, frequent maintenance works are generally required especially in unpaved roads. This effort can be minimized by the construction of a low cost surface layer of stabilized soil, which uses the local soil instead of the significant resources associated to the construction of a traditional pavement structure (Guedes, 2013).

Traditionally soils are stabilized with cement and/or lime (Szymkiewicz et al., 2012, Wang et al., 2015, Zhao et al., 2016), however, cement production has severe environmental impacts, using vast amounts of fossil fuels and being responsible for the emission of more than 5% of all the carbon dioxide worldwide (Provis and Deventer, 2014). Hence, the development of low carbon alternative binders using increasing amounts of waste materials has been encouraged (e.g., Consoli et al., 2007). For example, the use of lime and fly ash for soil improvement has been used for decades (Mateos and Davidson, 1962; Ghosh and Subarao, 2001; Consoli et al., 2011), but the activation of fly ash with an alkaline solution is far more effective providing much higher strength (Rios et al., 2016a).

As first described by Davidovits (1991), geopolymers result from the reaction of a solid aluminosilicate with a highly concentrated aqueous alkali hydroxide or silicate solution. The solid aluminosilicate dilutes in the alkaline solution, which leads to the formation of a gel. Then the system continues to reorganize, as the connectivity of the gel network increases, resulting

in the three-dimensional aluminosilicate network associated to geopolymers (Duxson et al., 2007). The results are highly improved if the aluminosilicate source has suffered a previous thermic treatment (Xu and van Deventer, 2003) such as slags, ashes, metakaolin, among others.

Geopolymers have been studied for different applications within the construction industry, namely looking in detail to the properties of cement, mortars and concrete (e.g., Fernandez-Jimenez et al., 2005; Duxson et al., 2007; Bernal et al., 2011; Abdollahnejad et al., 2015; Tahri et al., 2015). More recently, there are also some works about alkali-activated cements (AAC) for soil improvement applications, where the authors tried to overcome the disadvantages of curing at ambient temperature and the interaction with the local soil. For example, Obana et al. (2012) and Yi et al. (2015) dealt with marine sediments, Sukmak et al. (2013), Cristelo et al. (2011, 2013) and Peirce et al. (2015) worked with clays, and Zhang et al (2013), Rios et al. (2016b) and Phummiphan et al. (2016) used other soils. Depending on the envisaged application and local soil, the challenges are different conversely to what happens in cement, mortars and concrete. For that reason, more research is needed in this area since there are still some issues not completely well understood. Although, a significant improvement in time has been recognized with significant improvements between the 28^{th} and 90^{th} day mark (Rios et al., 2016b), the early age strength and its evolution at long term (after 180 days) is very dependent on the type of aluminosilicate source, type and concentration of alkaline solution and liquid/solids ratio (Messina et al., 2015). Cristelo et al. (2013) showed that there is a strong dependency between the activator/ash ratio and mechanical strength, being an important key parameter for these mixtures.

This paper pretends to contribute to the increasing knowledge of AAC for soil improvement focusing on the long term behaviour, on the resistance to immersion, and on the resistance to wetting and drying cycles, which are required properties for the specific application of unpaved

roads. Moreover, other parameters usually needed in road design were evaluated such as compression and tensile strength, CBR values, and swelling behaviour. For that purpose, existing European standards and specifications developed for soil-cement sub-base layers were used and discussed.

Experimental program

Materials

The results presented in this paper concern the stabilization of a Colombian soil classified as a silty sand (SM) according to the unified classification system (ASTM D 2487, 2011). The soil was collected in a quarry site called "El Cajón de Copérnico" located in Soacha in the south of Bogotá. The results of identification tests performed on this soil are summarized in Table 1 and the grain size distribution curve determined by sieving and hydrometer analysis according to ASTM D 422 (1998) is presented in Figure 1. It is a silty sand with non plastic fines, and low sand content, which does not fulfil the Colombian specifications for roads.

The fly ash (FA) used in the alkaline activation was produced by a Portuguese coal-fired thermo-electric power plant. Its particle size distribution curve (Figure 1) was determined by laser diffraction, using an analyzer from *Beckman Coulter*. Figure 1 also shows the grain size distribution curves of the two mixtures of soil with 10% and 20% of fly ash from which uniformity coefficients (C_U) of 175 and 96 were respectively deduced. This reduction on the uniformity coefficients due to the introduction of fly ash, results in lower Proctor densities as explained further below.

SEM micrographs of the soil and fly ash particles are shown in Figure 2 (a) and (b) respectively, and the results from EDS semi-quantitative chemical analyses are shown in Table 2. Although

both soil and fly ash are composed mainly by silica and alumina, the amorphous structure of the fly ash makes it much more reactive with the alkaline solution, while the soil almost does not take part of the reaction. From the chemical analysis, it is also possible to identify the low calcium content of the fly ash, which was therefore classified as Class F according to ASTM C 618 (2015). EDS spectra was collected during at least 10 minutes using an EDAX equipment. A Dead Time (DT) of 33% was used, with typical 2000 Counts/s. The Live time was 500 s. Quantitative analysis was performed in ZAF standardless mode.

The alkaline activator solution was made by mixing a commercial sodium silicate (SS) solution ($Na_2Si_3O_7$) with a sodium hydroxide (SH) solution (NaOH) prepared to the desired concentration by dissolving sodium hydroxide pellets in water. The SS solution has a bulk density of 1.464 g/cm^3 at 20ºC, a SiO_2/Na_2O weight ratio of 2.0 (molar oxide ratio of 2.063) and a Na_2O concentration in the solution of 13.0%. The SH pellets have a specific gravity of 2.13 at 20ºC (99 wt%).

Mixtures definition

The compaction conditions of the treated soil mixtures were based on the modified Proctor tests performed over specimens of soil, fly ash and water. Since Proctor tests give parameters for the compaction of the treated soil immediately after mixing, i.e. without curing, it was considered that the presence of the activator was not very relevant for the purpose of defining the compaction conditions and so the Proctor tests were performed with water. Two fly ash percentages, of 10% and 20% of the dry soil, were adopted and modified Proctor curves were obtained for each case as illustrated in Figure 3. It is clear that the maximum dry unit weight reduced with the amount of fly ash. This can be explained by the uniformity coefficients

presented above because well graded soils (with higher C_U values) are able to compact more and therefore achieve higher values of maximum dry unit weight.

From the results of Figure 3, two sets of mixtures were defined, one with 10% of fly ash (A series) and another with 20% of fly ash (B series) both compacted to their optimum compaction points (10% of FA: γ_d=19.92 kN/m^3 and w=8%; 20% of FA: γ_d=19.53 kN/m^3 and w=8.8%). However, in these new mixtures the liquid phase is no longer just composed by water (as in Proctor tests) but by an alkaline solution. For that reason, in the mixtures preparation the water content was replaced by the liquid content defined as a liquids/solids ratio.

For each set of mixtures, two sodium silicate to sodium hydroxide ratios (in weight) of 0.5 and 1.0 were considered (SS/SH), as well as 4 molal concentrations of sodium hydroxide (5, 7.5, 10 and 12.5 molal), comprising 16 types of mixtures. Each mixture was identified as follows: A or B depending on the fly ash content and corresponding compaction point; 05 or 1 depending on the SS/SH ratio of 0.5 or 1.0; and the C5, C7, C10 or C12 depending on the NaOH concentration of 5, 7.5, 10 or 12.5 molal (Table 3).

Additionally, untreated specimens prepared only with soil and water; or soil, water and fly ash were also moulded for comparison purposes as indicated in the first three lines of Table 3. In this case, an average value of the compaction conditions of these untreated specimens was adopted so that the results could be compared.

Specimen preparation and testing procedures

The mixture was prepared by mixing the necessary quantities of soil, fly ash, sodium silicate solution, sodium hydroxide pellets and water. Since dissolution of SH pellets in water is a

highly exothermic reaction the solution was prepared in the day before to allow sufficient time to cool down to the room temperature. In the moulding day the soil and fly ash were first mixed until complete homogenization and then the activator solution was prepared by mixing the SS solution with the SH solution of the previous day. Finally, the solids (soil and fly ash) were manually mixed with the alkaline solution until a homogeneous paste was obtained.

The mixture was then statically compacted in a lubricated stainless steel mould of 71 mm of diameter and 142 mm of height according to the procedure described in ASTM D 1632 (2007). Immediately after moulding, the specimens were removed from the mould, and their weight, height and diameter were carefully measured. Before placing the specimen in a controlled temperature room (20ºC) for curing, it was wrapped in cling film to avoid moisture loss.

The experimental plan comprises unconfined compression strength tests (UCS), indirect tensile strength tests (ITS), seismic wave measurements (Waves), Californian Bearing Ratio (CBR), wetting and drying tests (WD), resistance to immersion (IM) and expansion tests (EXP) performed in different curing periods as summarized in Table 4. UCS tests and seismic wave measurements were performed in all the treated soil mixtures for the evaluation of each component effect. The other tests were only performed in some selected mixtures taking into account the UCS and Waves results. Triaxial compression tests (Tx) with local strain instrumentation were performed in the soil, soil+10% of fly ash mixtures without curing, as well as in a selected mixture of treated soil at 28 days of curing period.

The unconfined compression tests and indirect tensile tests, performed according to ASTM D 1633 (2007) and ASTM D 1634 (1996), respectively, used an automatic load frame with displacement control and a load cell with 25 kN of capacity for specimens up to 28 days of curing and a load cell with 100 kN of capacity for specimens with more days of curing. In order

to evaluate the unload-reload stiffness during the UCS tests, small unload-reload cycles at 10% and 25% of the expected maximum strength were performed and local strain instrumentation by means of Hall-Effect transducers was used in all tests. For that reason, the tests were performed at 0.05 mm/min, a slower speed than the indicated in the standard.

Seismic wave measurements were performed to monitor the curing process by accessing the elastic stiffness increase with time. Being a fast, non-destructive and reliable testing method it allows a good monitoring of a great number of specimens in a feasible time, conversely to strength tests which require a great amount of similar specimens to be tested at different curing periods. It comprises the evaluation of P and S wave propagation times with ultrasonic transducers as described in detail in Rios et al. (2016c). These transducers are more convenient than bender elements (e.g., Ferreira et al., 2011) when used in very stiff materials such as cemented soils (Molero et al., 2011), because it is not necessary to perform a small incision to insert the bender element. Due to the great stiffness and strength of the specimens even with few curing days, an incision with the exact bender size allowing a good coupling was very difficult to execute. Measurements were made at frequencies of 24, 37, 54, 82 kHz and the propagation time was identified in the signal that showed better amplification since it is assumed that wave velocity is frequency independent for the range of frequencies applied (e.g., Lee and Santamarina, 2005). The equipment set up includes a pair of compression transducers with 82 kHz of nominal frequency, a pair of shear transducers with nominal frequency of 100 kHz, a pulse waveform generator and data acquisition unit equipped with an amplifier connected to a personal computer with specific software to operate as an oscilloscope. Test measurements were made along the longitudinal axis of the cylindrical specimen placing the transmitter in the bottom of the specimen and the receiver on the top. To improve the acoustic coupling between transducers and the specimen, ultrasonic conductive gel was used. The results presented below correspond to the average of at least 10 consecutive pulse velocity readings.

The CBR tests were performed in the Central Laboratory (LABC) of MOTA-ENGIL, which is Quality Certified (nº L0315, 2003) by IPAC (Portuguese Accreditation Institute) in accordance with standard EN ISO/IEC 17025 (CEN, 2005). To obtain the CBRe values following ASTM D 1883 (1999), three test specimens were prepared according to the previously executed Modified Proctor test, considering the optimum moisture content and compacted with 55, 25 and 12 blows, which led to relative compaction levels between 90 and 100%. After a 96h period of saturation, the 3 specimens were subjected to the CBR tests and from these results CBR related with 95% of relative compaction was interpolated. Additionally, immediate CBR tests (CBRi) were also performed according to NF P 94-078 (AFNOR, 1997). In the case of soil and soil+fly ash mixtures the tests were performed after moulding, while in the case of treated mixtures, the tests were performed at 28 days of curing time.

The expansion test consisted in a large mould of 152.14 mm of diameter and 100 mm height where the specimen was compacted and its height was monitored during 56 days.

The wet and drying tests (WD) following NBR 13554 (ABNT, 2012) give an idea of the durability of the material as a capping layer of an unpaved low cost road (Guedes et al., 2015). Following the French specification for stabilized soils with hydraulic binders in embankments and capping layers (LCPC, 2000), some tests were executed to evaluate the short term strength and the resistance to immersion (IM). As the mixtures showed good behaviour in the immersion tests, another set of tests was performed as described below.

The triaxial compression tests followed the usual procedure: water percolation up to 150-300 ml; saturation up to 500 kPa of back-pressure at a rate of 30 kPa/h; consolidation at 30 kPa/h up to the desired effective confining pressure, and shear controlled by displacement

in a load frame equipped with a load cell of 10 kN for the tests with unbounded soil and 50 kN for the tests with "treated soil".

Results

Unconfined compression and tensile strength

The 16 mixtures specified in Table 3 were subjected to unconfined compression strength tests at 28 days to evaluate the best composition for this particular soil. Three specimens of each mixture were moulded and tested in order to have 3 strength measurements for each case. The results presented in Figure 4show a considerable increase in strength comparing to unbound soil specimens. Mixtures containing 10% of fly ash (A series) have generally lower strength than the mixtures with 20% of fly ash (B series) but are less expensive. In fact, an integrated analysis of cost and strength was made to evaluate the best mixture, which is also expressed in Figure 4. The cost is also associated to the carbon footprint, as higher fly ash content results in a higher quantity of activator, which is more expensive and produces more greenhouse emissions. Giving these results, two mixtures from the less expensive series (10% of fly ash) were selected for the following tests: A05C7 and A1C7. They are both with 7.5 molal concentration because the 5 molal did not show very good results indicated by a higher scatter and some fissures in the specimens that do not give confident results, and the other concentrations are more expensive and do not show a significant increase in strength.

In fact, in Figure 4 there is no direct correlation between the SH concentration and the UCS as it was expected from other published works (e.g., Xu and van Deventer, 2000; Cristelo et al., 2012). Alonso and Palomo (2001) and Hwang and Huynh (2015) have also reported some decrease in strength for NaOH concentration higher than 10 molal especially for low curing

temperatures, as it was the case of this study. Alonso and Palomo (2001) state that high activator concentrations produce high pH in the liquid phase which favours anionic forms of silicate delaying polymerization while if the stable form was the molecular one (ortosilicic acid) the polymerization reaction is favoured. Consequently, since higher concentrations may delay the polymerization process this reduction in strength with increasing concentration might be less evident when higher curing periods are considered. For that reason, some specimens (A1 series – 10% of fly ash and SS/SH = 1) prepared with different NaOH concentrations (7.5; 10 and 12.5 molal) were tested at 90 days of curing period. The results showed that the strength reduction with the increase of the molal concentration was also significant at 90 days (46% reduction) and even higher than at 28 days (30% reduction), conversely to what was expected from the literature. This reduction may be due to the alkali activated compositions used in this research study with low values of liquid/solids ratio in comparison with other published works from the literature working with soil-geopolymer mixtures cured at ambient temperature (Zhang et al., 2013; Cristelo et al., 2012, 2013). For this reason, further studies on their controlling variables are still needed since these are very much dependent on the type of mixture and curing conditions.

The UCS strength of the two selected mixtures was analyzed up to 360 days of curing as illustrated in Figure 5. Both mixtures show a good adjustment with a logarithmic law indicating that it is still evolving at 360 days. This continuous evolution with time, even beyond the 28 days reference, is the main difference of this binder in comparison with Portland cement as expressed by Rios et al. (2016b). In fact, the cementation between particles is clearly visible in SEM micrographs of treated specimens. Figure 6 presents the comparison between a treated specimen (A1C7) after 1 year of curing, with a similar specimen where the activator was replaced by water (i.e., uncemented), so the effect of the alkaline activator on the cementation can be properly observed. While the uncemented specimen shows the fly ash particles (with a

very rounded shape as presented in Figure 2b) just placed above the soil particles, in the treated specimen there is a clear bond between both materials. Please note that both micrographs of Figure 6 have the same scale for comparison purposes.

The results of indirect tensile strength tests are presented in Table 5 for the two selected mixtures: A05C7 and A1C7. Despite the two outliers (1 and 5), the relationship between indirect tensile strength and unconfined compression strength is around 7.5% for both mixtures, being a bit smaller than what has been observed in soil-cement tests (around 10% as reported by Rios and Viana da Fonseca, 2013).

These results allowed the comparison of this material behaviour with the classification chart proposed in LCPC (2000) and EN 14227-10 (CEN, 2006) based on the tensile strength and Young modulus. The tensile strength (R_t) was obtained, as indicated in this guide, by multiplying the indirect tensile strength reported in Table 5 by 0.8. The Young modulus (E) was obtained from the first unload-reload cycle performed in the UCS tests assumed to be elastic. Figure 7 shows the lines that separate the different classification zones for each standard. Although the tested mixtures do not fit within the higher classification zones with more tensile strength and stiffness, their performance is accepted as stabilized material for a capping layer. Please note that the selected mixtures were not the most well performing of Figure 4, so it is possible that other mixtures (such as B1C7) could fit in the higher classes. As in any other cemented material, the binder amount determines its cost and performance.

Dynamic stiffness evolution with curing

The same specimens tested in UCS tests at 28 days presented in Figure 4 were used for measuring P and S wave propagation time with ultrasonic transducers during the curing process.

315 The interpretation to identify the wave travel time (t) is based on time domain approach,
316 according to Viana da Fonseca et al. (2009). Wave velocities are then calculated dividing the
317 specimen length (which corresponds to the travel distance) by the corresponding travel time.
318
319 From the elasticity theory it is possible to obtain the maximum shear modulus (G_0), the
320 constrained modulus (M_0), the Young modulus (E_0) and the dynamic Poisson ratio (υ) according
321 to the following equations:

$$G_0 = \rho V_S^2 \quad (1)$$

$$M_0 = \rho V_P^2 \quad (2)$$

$$E_0 = 2G_0 (1 + \nu) \quad (3)$$

$$\nu = \frac{\left(\frac{V_P}{V_S}\right)^2 - 2}{2\left(\frac{V_P}{V_S}\right)^2 - 2} \quad (4)$$

322
323
324 Although different mixtures led to distinct stiffness absolute values, the Young modulus
325 evolution with time has a similar trend in a significant number of specimens following a
326 logarithmic trendline with similar exponent values, as illustrated in Figure 8. Following these
327 results, a unique relationship was obtained - equation (5) - normalizing each curve of Figure 8
328 by the corresponding Young modulus at 28 days (E_0^{28}) as shown in Figure 9. This relationship,
329 although with some scatter, is very interesting as it is independent of the mixture. Having E_0 at
330 28 days it is possible to calculate the E_0 for any mixture at a certain age without any more tests.

$$E_0 = E_0^{28} \cdot [0.24 \ln(t) + 0.15] \quad (5)$$

331
332
333 As explained in Table 4, seismic wave measurements were performed for two mixtures up to
334 360 days of curing time. Although the stiffness increase is very different in the two mixtures,

equation 5 adapts fairly well to both of them (Figure 10). The adjustment is almost perfect up to 30 days, which is reasonably since the normalization is done for 28 days. Moreover, it is also clear that for mixture A1C7 the stiffness is still increasing significantly up to 180 days of curing as observed for strength in Figure 5, which is in agreement with previous studies (eg. Rios et al., 2016c).

Based on the logarithmic law relating the dynamic stiffness evolution with time, a similar procedure was performed for the UCS results presented in Figure 5, which was compared to the dynamic stiffness relation – equation (5) - as presented in Figure 11.

Taking these results, these two expressions were combined and a unique linear relationship was found between stiffness and strength without the time parameter, indicating that both variables evolve in the same way.

$$\frac{E_0}{E_0^{28}} = 0.55 \cdot \left(\frac{UCS}{UCS_{28}} \right) + 0.4 \quad (6)$$

Short term strength and Resistance to immersion

According to LCPC (2000) the short term strength is evaluated by: the age for which the specimen has enough strength to support traffic considered higher than 1 MPa; and the resistance to immersion at early ages.

In the first case, the unconfined compression strength should be performed at 7 and 28 days and then the age for 1 MPa of strength is evaluated by interpolation. If the strength at 7 days is higher than 1 MPa, as it was the case, the interpolation should be done between 4 and 7 days. Table 6 shows the results obtained for the two mixtures at 4, 7 and 28 days and the age for UCS

of 1 MPa, showing that the specimens have a significant strength after a few days of curing. It is interesting to note that although these mixtures have a very long curing period, as it was illustrated in Figure 5 with a significant evolution of strength up to 360 days, this does not mean that the short term strength is small.

The resistance to immersion at early ages is evaluated, according to LCPC (2000), by the ratio between UCS_{i60}/UCS_{60} where UCS_{i60} is the unconfined compression strength of a specimen with 28 days of normal curing followed by 32 days fully covered by water, and UCS_{60} is the unconfined compression strength of a specimen with 60 days of normal curing. Although the water has become a bit blurred, both mixtures passed this test, presenting ratios higher than 0.8 (0.86 for A05C7 and 1.03 for A1C7) as recommended in LCPC (2000). The behaviour of these mixtures under water was important to evaluate since AAC and hydraulic binders have quite distinct chemical reactions. In soil-cement, Portland cement particles hydrate with water, i.e., the mixture retains part of the free water becoming part of the cemented mass. In opposition, according to the chemical reactions presented by Xu and van Deventer (2000), AAC release water during their formation, and so their curing in water could be affected. Moreover, the water could dilute the alkaline medium that favours the activation of fly ashes reducing the reaction extent. However, since the specimen was cured for 28 days before being introduced in water, the strength achieved during that period prevented a significant loss induced by the water, indicating that this material is suitable for roads with exposure to rain.

To evaluate the wetting effect on the specimen's strength at even earlier ages, a comparison between specimens with different curing times and immersion periods is shown in Figure 12. For both mixtures, results are presented for 7, 28 and 60 days. For 7 days, the specimens were not soaked in water. For 28 days there are two UCS values: one without immersion and other

corresponding to a specimen soaked at 7 days. For the 60 days, there is also a UCS value without immersion and another corresponding to a specimen soaked at 28 days.

The unconfined compression strength of the specimens tested at 28 days reduces when they are soaked in water at 7 days indicating that immersion affects the final resistance. In fact, the UCS values of the specimens tested at 28 days but soaked at 7 days, is similar to the UCS values at 7 days of normal curing (especially for A05C7), indicating that immersion almost stopped the strength development. However, in the specimens tested at 60 days of curing, the difference between UCS values of immersed and non immersed specimens is not so significant which is explained by the fact that at 28 days the specimens have reached considerable strength that prevents the specimen from being significantly affected by immersion.

[California Bearing Ratio tests

a) Additionally, the CBR values performed on the treated and untreated soil can give an idea of the short and long term performance of the material. The results presented in Table 7 show a stiff behaviour of the untreated soil with results of 60%, which decrease significantly with the introduction of fly ash (30 and 22% of CBR, respectively in mixtures with 10 and 20% of fly ash). In the treated mixtures (A05C7 and A1C7) both the usual CBRe (which includes a 4 days saturation) and immediate CBR (CBRi) were tested after 28 days of curing period. CBRe values of the treated soil are higher than the values obtained in soil-fly ash mixtures, but remain lower than the results obtained in the original soil, which reveals that the curing time was not enough to get the strength given by the treatment or, the immersion period had a significant effect on strength. In fact, the analysis of the data reveals a stiffness decrease with the presence of water, which seems to vary with SS/SH ratio. In fact, CBRe values show an increase in

stiffness for higher SS/SH, while for CBRi (without immersion) lower SS/SH ratios result in higher stiffness with more pronounced differences for higher compaction levels.

Resistance to wetting and drying cycles and expansion

Following NBR 13554 (ABNT, 2012) developed for soil-cement, the weight losses, water content changes, and volume changes (swell and shrinkage) produced by repeated wetting and drying of hardened specimens were evaluated. For each mixture, 3 specimens were moulded: the first was to obtain the changes in water and volume during the wetting and drying cycles while the other two were used to obtain the specimen losses due to brushing stokes with a wire scratch brush. The specimens were placed in water on the 7^{th} day of curing, following cycles of 5 h in water and 42 h in oven (71+/- 2ºC). The first specimen revealed that, conversely to what happens in soil-cement, the water was not retained in the specimens during the cycles. This is explained by the AAC characteristics described above. The AAC reactions involve loss of water, and therefore the average water retained, as required by the standard, is negative. The other two specimens, that followed the same cycles plus the brushing, also reported loss of mass, which should correspond to the loss of water (like specimen 1) and loss of soil due to brushing. Removing the loss of water suffered by specimen 1, the loss of mass due to brushing can be obtained. The maximum value obtained in both specimens was 1.58% indicating that brushing does not produce significant degradation to the specimen, in agreement with the results obtained by Guedes et al. (2015) in soil-cement specimens. This is surprising because the specimen surface is not very smooth having big soil grains that could be easily removed by the brush. Since the mass loss was not very significant, it means that the alkali activated cement that links the soil particles is relatively strong.

After performing the cycles, the specimens were dried in the oven (105-110ºC) until constant mass, and then tested in unconfined compression, so their strength was compared to similar specimens subjected to normal curing. The results show that the specimens that followed the wetting and drying cycles have higher strength than the ones that followed the normal curing. This was expected since the geopolymeric reactions are highly accelerated with temperature increase (e.g., Sukmak et al., 2013).

The volume change (evaluated in the first specimen that followed the wetting and drying cycles but not the brushing stokes) was also reduced, below 1.4%, indicating that there is not significant expansion in water or shrinkage due to curing process. However, to have a quantitative evaluation, an expansion test in normal curing conditions was performed in A05C7 mixture as described previously. The variation in the specimen height was measured during 2 months, but no significant expansion was recorded since the maximum vertical expansion was 0.62%.

Stress-strain behaviour and strength envelope

Triaxial compression tests with local strain measurements by means of Hall-effect transducers were performed in the soil, soil with 10% and 20% of fly ash (without alkaline activator thus, without cementation), as well as in mixture A1C7 at 28 days here identified as "treated soil". The confining pressures of these tests were 50, 300 and 600 kPa for the tests with soil and, soil with fly ash and 50, 100 and 150 kPa for the tests with "treated soil" in order to avoid damaging the cementation structure.

As illustrated in Figure 13 for 50 kPa confining pressure, the treated soil shows a very stiff stress-strain curve, conversely to the soil and soil-ash mixtures, associated to a brittle failure

followed by strain softening, as it is typical of cemented materials (Rios et al., 2014). This is related to a high degradation rate of the stiffness degradation curve after bound breakage, observed in this particular case by the ratio between the dynamic stiffness modulus (E_0) and the initial secant modulus (E_{sec}), obtained from the triaxial test with smaller confining stress (50 kPa), which is almost constant up to peak: $E_0/E_{sec} = 6088/551 = 11$.

It is also observed that the addition of fly ash to the soil slightly reduces the peak strength, which might be related to the specimen lower dry unit weight, considered the optimum modified Proctor value illustrated in Figure 3. This lower optimum density is in agreement with the uniformity coefficients (C_u) since these values reduced with the introduction of fly ash as explained above. However, the use of the alkaline solution largely compensates this, since the treated soil has achieved more than ten times the soil (and soil-ash) strength. This is also clear in the obtained strength envelopes presented in Figure 14. The treated soil shows very high angles of shearing resistance due to high dilatancy angles but also a significant increase in the cohesion intercept as a sign of cementation.

Discussion

An extensive experimental program was developed to analyse the behaviour of a Colombian soil stabilized with AAC. The aim was to evaluate the performance of this material in different curing conditions regarding its possible application in an unpaved road. The evolution of strength and stiffness with time, which is different from the well-known soil-cement due to the chemical reactions involved in the AAC curing process, have consequences in terms of the material performance, which needed a careful study. For that purpose several tests were performed, first in a great number of mixtures and afterwards in mainly two selected mixtures. Instead of selecting the specimens that showed higher strength, weaker mixtures resulting from

lower concentrations of the alkaline solution were selected to observe the lower bound limitations of this technique. This is very important because using a low quantity of activator not only reduces the cost of the mixtures but also their carbon footprint. In that sense, distinct tests recovered from specifications and standards available for soil-cement were used to evaluate the short term strength, the resistance to immersion, the resistance to wetting and drying cycles, strength and dynamic stiffness parameters, among others.

It has been observed that the key variables that, according to other authors (e.g., Xu and vanDeventer, 2000; Rashad and Zeedan, 2011; Cristelo et al., 2012), should rule the AAC performance (such as the NaOH concentration) do not have the same influence in the mixtures reported in this paper. While the literature works report an increase in strength with NaOH concentration, in the present study this was not clear. This may be due to the much lower liquid/solids ratio of these mixtures, making them particularly sensitive to other key variables such as viscosity. In fact, while in grout mixtures, the increase in the concentration of the alkaline solution (affecting viscosity and workability) does not prevent the strength increase; in a much drier mixture, this may have a significant impact. For this reason further studies involving the development of rational dosage methodologies based on well-defined controlling variables as exists for soil-cement (e.g., Rios et al., 2014) are of major importance. In the case of AAC-soil mixtures the key variables may be the solids/liquid ratio, the ratio between ash and activator, or the ratio between the two components of the activator.

The tests on the resistance to immersion showed that if the material is submerged very early (for example, at 7 days of curing) there is a significant impact on the final strength since it does not evolve much beyond the early age strength value. On the contrary, if the material is submerged in water at larger ages (for example at 28 days) the impact is almost negligible. These results were in agreement with CBR tests, since the CBRe values were found to be lower

than the CBRi for the treated specimens, especially in the weaker mixtures. This happens because the AAC reactions involve the loss of water from the specimen, which are not favoured when placed under water. On the other hand, it is admitted that the presence of water may reduce the concentration of the alkali ions in the gel changing its properties and its ability to harden. However, in the wetting and drying cycles of NBR 13554 (ABNT, 2012) the loss of strength that the immersion in water at early ages might cause was compensated by the increase in strength caused by the curing periods in the oven. As reported by several authors (e.g., Duxson et al., 2007), the AAC reactions are very much affected by temperature, being specially accelerated with temperatures above 85ºC.

For the mild temperatures of the laboratory, around 20ºC, the strength parameters obtained for the selected mixture in saturated conditions show high angles of shearing resistance and cohesion intercepts typical of cemented materials, high above the values obtained by the soil itself.

Conclusions

This paper highlights some important properties of a soil treated with AAC, summarized in the following:

- Although the increase of strength and stiffness in time is very significant, following a logarithmic law far beyond the usual 28 days observed in materials treated with hydraulic binders, the short term strength (7 days) is still above the 1 MPa, considered the necessary strength to support vehicle circulation;
- Immersion at early ages may affect the curing process, actively reducing the final strength, except if compensated by high temperatures that fasten the curing process;
- Stress-strain curves and strength parameters are typical of cemented soils.

- Further studies are needed to evaluate how the key parameters that rule the AAC grouts (such as the activator type and concentration, the Na_2O/ash ratio, the Si/Al ratio, or the solids/liquid ratio) affect the performance of soils treated with AAC. The present results indicate that existing relations may act differently in this case.
- Although other studies are still needed, the results presented in this paper encourage the use of this material in unpaved roads especially if applied in warmer climates and if compacting the capping layer in the dry season.
- These technique will be also more competitive in coal producing countries (which have a great amount of fly ash to dispose) and with lack of calcareous materials for cement production.

Acknowledgements

This work was executed under the project ECOLOSO (reference FCOMP-01-0202-FEDER-038899), funded by the European Fund for Regional Development (FEDER), through the Operational Program for Competitiveness Factors (POFC) of the National Strategic Reference Framework (QREN), on the scope of the incentive system for research and technological development. The authors would also like to acknowledge the Chemical Engineering Department of University of Porto, namely Professors Fernão Magalhães and Adélio Mendes, for the use of the Particle Size Analyser; the company Pegop – Energia Eléctrica SA which runs the thermoelectric power plant of Pego, for the supply of fly ash; and the MCTES/FCT (Portuguese Science and Technology Foundation of Portuguese Ministry of Science and Technology) for their financial support through the SFRH/BPD/85863/2012 scholarship, which is co-funded by the European Social Fund by POCH program.

References

Abdollahnejad, Z., S. Miraldo, F. Pacheco-Torgal and J. B. Aguiar (2015). Cost-efficient one-part alkali-activated mortars with low global warming potential for floor heating systems applications. *European Journal of Environmental and Civil Engineering*, 1-18.

ABNT NBR 13554:2012 (2012). Soil-cement - wetting and drying tests - Method of test. Associação Brasileira de Normas Técnicas (in Portuguese)

AFNOR NF P 94-078 (1997). CBR index after immersion. Association Française de Normalisation, Paris, France

Alonso, S. and A. Palomo (2001). Alkaline activation of metakaolin and calcium hydroxide mixtures: influence of temperature, activator concentration and solids ratio. *Materials Letters, 47*(1–2), 55-62. DOI: 10.1016/S0167-577X(00)00212-3

ASTM D 422 (1998). Standard test method for particle size analysis of soils. ASTM Int. Annu. B. Stand, Vol. 04.08, 1–8.

ASTM C 618 (2015). Standard specification for coal fly ash and raw or calcined natural pozzolan for use in concrete. ASTM Int. Annu. B. Stand, Vol. 04.02, 1–5.

ASTM D 1632 (2007). Standard practice for making and curing soil-cement compression and flexure test specimens in the laboratory. ASTM Int. Annu. B. Stand. Vol. 04.08, 1–5.

ASTM D 1633 (2007). Standard Test Methods for Compressive Strength of Molded Soil-Cement Cylinders. ASTM Int. Annu. B. Stand. Vol. 04.08, 1–5.

ASTM D 1634 (2000). Standard Test Method for Compressive Strength of Soil-Cement Using Portions of Beams Broken in Flexure (Modified Cube Method). ASTM Int. Annu. B. Stand, Vol. 04.08, 1–5.

ASTM D 1883 (2016). Standard Test Method for California Bearing Ratio (CBR) of Laboratory-Compacted Soils. ASTM Int. Annu. B. Stand, Vol. 04.08, 1–5.

ASTM D 2487-2006 (2011). Standard practice for classification of soils and engineering purposes (Unified Classification System), ASTM Int. Annu. B. Stand. Vol. 04.08, 1–5.

Bernal, S., R. M. Gutiérrez, A. L. Pedraza and J. L. Provis (2011). Effect of binder content on the performance of alkali-activated slag concretes. *Cement and concrete research, 41*, 1-8. DOI: 10.1016/j.cemconres.2010.08.017

Brito, L. (2011). Design methods for low cost roads. PhD thesis submitted to the University of Nottingham, United Kingdom.

CEN (2005). EN ISO/IEC 17025. General requirements for the competence of testing and calibration laboratories. Comité Européen de Normalisation, Brussels

CEN (2006). EN 14227-10 - Mélanges Traités Aux Liants Hydrauliques - Spécifications - Partie10: Sol Traité Au Ciment, Comité Européen de Normalisation, Brussels

Consoli, N., K. Heineck, M. Coop, A. Viana da Fonseca and C. Ferreira (2007). Coal bottom ash as a geomaterial: influence of particle morphology on the behaviour of granular materials. *Soils and Foundations, 47*(2), 361-373. DOI: 10.3208/sandf.47.361

Consoli, N., Dalla-Rosa, A., & Saldanha, R. (2011). Variables Governing Strength of Compacted Soil-Fly Ash-Lime Mixtures. *Journal of Materials in Civil Engineering, 23*(4), 432-440. DOI: 10.1061/(ASCE)MT.1943-5533.0000186

Cristelo, N., S. Glendinning and A. Teixeira Pinto (2011). Deep soft soil improvement by alkaline activation. *Ground Improvement, 164(GI2)*, 73-82. DOI: 10.1680/grim.900032

Cristelo, N., S. Glendinning, T. Miranda, D. Oliveira and R. Silva (2012). Soil stabilisation using alkaline activation of fly ash for self-compacting rammed earth construction. *Construction and Building Materials, 36*, 727-735. DOI: 10.1016/j.conbuildmat.2012.06.037

Cristelo, N., S. Glendinning, L. Fernandes and A. Teixeira Pinto (2013). Effects of alkaline-activated fly ash and Portland cement on soft soil stabilisation. *Acta Geotechnica*, 8, 395-405. DOI: 10.1007/s11440-012-0200-9

Davidovits, J. (1991). Geopolymers - Inorganic polymeric new materials. *Journal of Thermal Analysis*, 37,1633-1656.

Duxson, P., A. Fernandes-Jiménez, J. L. Provis, G. C. Luckey, A. Palomo and J. S. J. van Deventer (2007). Geopolymer technology: the current state of the art. *Journal of Materials Science, 42*, 2917-2933.

Fernández-Jiménez, A., A. Palomo and M. Criado (2005). Microstructure development of alkali-activated fly ash cement: a descriptive model. *Cement and Concrete Research*, 35, 1204-1209. DOI: 10.1016/j.cemconres.2004.08.021

Ferreira, C., Viana da Fonseca, A., Nash, D. (2011). Shear wave velocities for sample quality assessment on a residual soil. *Soils and Foundations*, 51(4), 683-692. DOI: 10.3208/sandf.51.683

Fukubayashi, Y. and M. Kimura (2014). Improvement of rural access roads in developing countries with initiative for self-reliance of communities. *Soils and Foundations*, 54(1), 23-35. DOI: 10.1016/j.sandf.2013.12.003

Ghosh, A., & Subbarao, C. (2001). Microstructural development in fly ash modified with lime and gypsum. *Journal of Materials in Civil Engineering*, 13(1), 65–70 DOI:10.1061/(ASCE)0899-1561(2001)13:1(65), 65-70.

Guedes, S. (2013). Mechanical behavior of soil-cement reinforced with synthetic fibers for low cost roads. PhD thesis submitted to the Federal University of Pernambuco, Recife, Brasil (in Portuguese).

Guedes, S., Coutinho, R. and Viana da Fonseca, A. (2015). Criteria to evaluate the cement content in a soil for a pavement base course. *Geotecnia*, 134, 127-145 (in Portuguese)

Hwang, C.-L. and T.-P. Huynh (2015). Effect of alkali-activator and rice husk ash content on strength development of fly ash and residual rice husk ash-based geopolymers. *Construction and Building Materials*, 101, Part 1: 1-9. DOI: 10.1016/j.conbuildmat.2015.10.025

LCPC (2000). Guide technique pour le traitement des sols à la chaux et/ou aux liants hydrauliques. Application à la réalisation des remblais et des couches de forme. (Technical guide for soils treated with lime and cement, In French), Laboratoire Central des Ponts et Chaussés (LCPC/SETRA).

Lee, J., Santamarina, J. (2005). Bender elements: Performance and signal interpretation. *Journal of Geotechnical and Geoenvironmental Engineering*, 131(9), 1063-1070. DOI: 10.1061/(ASCE)1090-0241(2005)131:9(1063)

Mateos, M. & Davidson, D. T. 1962. Lime and fly ash properties in soil-lime stabilization. *Highway Research Board Bulletin* No 335, 40-64.

Messina, F., C. Ferone, F. Colangelo and R. Cioffi (2015). Low temperature alkaline activation of weathered fly ash: Influence of mineral admixtures on early age performance. *Construction and Building Materials*, 86, 169-177. DOI:10.1016/j.conbuildmat.2015.02.069

Molero, M., I. Segura, S. Aparicio and J. V. Fuente (2011). Influence of aggregates and air voids on the ultrasonic velocity and attenuation in cementitious materials. *European Journal of Environmental and Civil Engineering*, 15(4), 501-517.

Obana, M., D. Levacher and P. Dhervilly (2012). Durability properties of marine sediments stabilised by pozzolan and alkali-activated binders. *European Journal of Environmental and Civil Engineering*, 16(8), 919-926.

Peirce, S., L. Santoro, S. Andini, F. Montagnaro, C. Ferone and R. Cioffi (2015). Clay sediment geopolymerization by means of alkali metal aluminate activation. *RSC Advances* 5(130), 107662-107669.

Phummiphan, I., S. Horpibulsuk, P. Sukmak, A. Chinkulkijniwat, A. Arulrajah and S.-L. Shen (2016). Stabilisation of marginal lateritic soil using high calcium fly ash-based geopolymer. *Road Materials and Pavement Design*. DOI: 10.1080/14680629.2015.1132632

Provis, J., Deventer, J. van (Eds.). (2014). Alkali Activated Materials: State-of-the-art Report, RILEM TC 224-AAM. Springer.

Rashad, A. and Zeedan, S. (2011). The effect of activator concentration on the residual strength of alkali-activated fly ash pastes subjected to thermal load. *Construction and Building Materials, 25*(7), 3098-3107

Rios, S. and Viana da Fonseca, A. (2013). Porosity/cement index to evaluate geomechanical properties of an artificial cemented soil. Proceedings of the 18th International Conference on Soil Mechanics and Geotechnical Engineering, 2589-2592, Paris

Rios, S., Viana da Fonseca, A. and Baudet, B. (2014). On the shearing behaviour of an artificially cemented soil. *Acta Geotechnica*, 9(2), 215-226, DOI: 10.1007/s11440-013-0242-7

Rios, S., Cristelo, N., Miranda, T., Araújo, N., Oliveira, J. (2016a). Increasing the reaction kinetics of alkali activated fly ash binders for stabilisation of a silty sand pavement sub-base. *Road Materials and Pavement Design,* 1-22, DOI: 10.1080/14680629.2016.1251959

Rios, S., Cristelo, C., Viana da Fonseca, A., Ferreira, C. (2016b). Structural Performance of Alkali Activated Soil-Ash versus Soil-Cement. *Journal of Materials in Civil Engineering*, 28(2) DOI: 10.1061/(ASCE)MT.1943-5533.0001398.

Rios, S., Cristelo, C., Viana da Fonseca, A., Ferreira, C. (2016c). Small and large strain behavior of soil-geopolymer versus soil-cement. *International Journal of Geomechanics* doi: 10.1061/(ASCE)GM.1943-5622.0000783

Sukmak, P., S. Horpibulsuk and S.-L. Shen (2013). Strength development in clay–fly ash geopolymer. *Construction and Building Materials*, 40, 566-574. DOI: 10.1016/j.conbuildmat.2012.11.015

Szymkiewicz, F., A. Guimond-Barrett, A. L. Kouby and P. Reiffsteck (2012). Influence of grain size distribution and cement content on the strength and aging of treated sandy soils. *European Journal of Environmental and Civil Engineering*, 16(7), 882-902.

Tahri, W., Z. Abdollahnejad, J. Mendes, F. Pacheco-Torgal and J. B. de Aguiar (2016). Cost efficiency and resistance to chemical attack of a fly ash geopolymeric mortar versus epoxy resin and acrylic paint coatings. *European Journal of Environmental and Civil Engineering,* 1-17.

Viana da Fonseca, A., Ferreira, C., and Fahey, M. (2009). A Framework Interpreting Bender Element Tests, Combining Time-Domain and Frequency-Domain Methods. *Geotechnical Testing Journal*, 32(2), 1-17, DOI: 10.1520/GTJ100974.

Wang, D., N. E. Abriak and R. Zentar (2015). One-dimensional consolidation of lime-treated dredged harbour sediments. *European Journal of Environmental and Civil Engineering*, 19(2), 199-218.

Xu, H. and J. S. J. van Deventer (2000). The geopolymerization of alumino-silicate minerals. *International Journal of Mineral Processes,* 59, 247-266.

Yi, Y., C. Li and S. Liu (2015). Alkali-Activated Ground-Granulated Blast Furnace Slag for Stabilization of Marine Soft Clay. *Journal of Materials in Civil Engineering*, 27(4), DOI: 10.1061/(ASCE)MT.1943-5533.0001100

Zhang, M., H. Guo, T. El-Korchi, G. Zhang and M. Tao (2013). Experimental feasibility study of geopolymer as the next-generation soil stabilizer. *Construction and Building Materials*, 47, 1468-1478. DOI: 10.1016/j.conbuildmat.2013.06.017

Zhao, H., K. Zhou, C. Zhao, B.-W. Gong and J. Liu (2016). A long-term investigation on microstructure of cement-stabilized handan clay. *European Journal of Environmental and Civil Engineering*, 20(2), 199-214.

Tables

Table 1. Physical properties of the soil

Plastic Limit (W_P)	NP
Liquid Limit (W_L)	NP
Mean effective diameter (D_{50})	0.20 mm
Specific gravity (G)	2.64
Fines content (<0.074 mm)	27.9 %
Uniformity Coefficient (C_U)	210
Curvature Coefficient (C_C)	8.60
Maximum dry unit weight for modified Proctor compaction effort (γ_d^{opt})	20.13 kN/m^3
Optimum water content for modified Proctor compaction effort (w^{opt})	8.6 %

Table 2. Composition of the soil and fly ash (wt%)

Element	SiO_2	Al_2O_3	Fe_2O_3	CaO	K_2O	TiO_2	MgO	Na_2O	SO_3	Others
Soil	80.33	11.41	3.62	-	2.81	0.89	0.27	-	-	0.67
Fly ash	54.84	19.46	10.73	4.68	4.26	1.40	1.79	1.65	0.7	0.5

Table 3. Mixtures composition

Mixture name	% Fly ash	Dry unit weight (kN/m^3)	Liquid content (%)	SS/SH (wt)	SH concentration (molal)
Soil	0	19.86	8.5	0	0
Soil10FA	10	19.86	8.5	0	0
Soil20FA	20	19.86	8.5	0	0
A05C5	10	19.92	8.0	0.5	5
A05C7	10	19.92	8.0	0.5	7.5
A05C10	10	19.92	8.0	0.5	10
A05C12	10	19.92	8.0	0.5	12.5
A1C5	10	19.92	8.0	1	5
A1C7	10	19.92	8.0	1	7.5
A1C10	10	19.92	8.0	1	10
A1C12	10	19.92	8.0	1	12.5
B05C5	20	19.53	8.8	0.5	5
B05C7	20	19.53	8.8	0.5	7.5
B05C10	20	19.53	8.8	0.5	10
B05C12	20	19.53	8.8	0.5	12.5
B1C5	20	19.53	8.8	1	5
B1C7	20	19.53	8.8	1	7.5
B1C10	20	19.53	8.8	1	10
B1C12	20	19.53	8.8	1	12.5

Table 4. Experimental plan

	Test name	UCS	Waves	UCS and Waves	UCS and Waves	UCS	EXP	CBR	ITS	WD	IM	Tx
	Curing time (days)	28	7, 14, 21 and 28	56 and 90	180 and 360	4 and 7	up to 56	28	28	28	(2)	28
Mixture name	Soil	X(1)										X(1)
	Soil10FA											X(1)
	Soil20FA											X(1)
	A05C5	X	X									
	A05C7	X	X	X	X	X	X	X	X	X	X	
	A05C10	X	X									
	A05C12	X	X									
	A1C5	X	X									
	A1C7	X	X	X	X	X		X	X	X	X	X
	A1C10	X	X	X								
	A1C12	X	X	X								
	B05C5	X	X									
	B05C7	X	X									
	B05C10	X	X									
	B05C12	X	X									
	B1C5	X	X									
	B1C7	X	X									
	B1C10	X	X									
	B1C12	X	X									

(1) In the unbounded soil specimens the tests were performed at 0 days since there is no curing process

(2) Defined in the text

Table 5. Indirect tensile strength tests

Specimen	ITS (MPa)	ITS/ UCS
A05C7_1	0.28	10.4%
A05C7_2	0.19	7.0%
A05C7_3	0.21	7.8%
A1C7_4	0.30	7.2%
A1C7_5	0.22	5.3%
A1C7_6	0.33	7.9%

Table 6. Short term strength: age for UCS = 1 MPa

Mixture	UCS at 4days (MPa)	UCS at 7days (MPa)	UCS at 28days (MPa)	Age for UCS = 1 MPa
A05C7	0.77	1.21	2.70	6 days
A1C7	0.88	1.22	4.17	5 days

737

738 Table 7. CBR values

		Untreated soil			Treated mixtures	
		Soil	Soil + 10% fly ash	Soil + 20% fly ash	A05C7	A1C7
CBRe	2.5mm a 95% CR	59%	29%	22%	31%	50%
	5.0mm a 95% CR	61%	31%	23%	28%	51%
	Expansion (95% CR)	0%	0%	0%	1%	1%
CBRi 55 blows	(2.5 mm)	-	-	-	112%	89%
	(5 mm)	-	-	-	116%	94%
CBRi 25 blows	(2.5 mm)	-	-	-	64%	44%
	(5 mm)	-	-	-	65%	47%
CBRi 12 blows	(2.5 mm)	-	-	-	37%	39%
	(5 mm)	-	-	-	38%	37%

739 (*) CR means the compaction relative to the Modified Proctor test

740

741

742

Figures

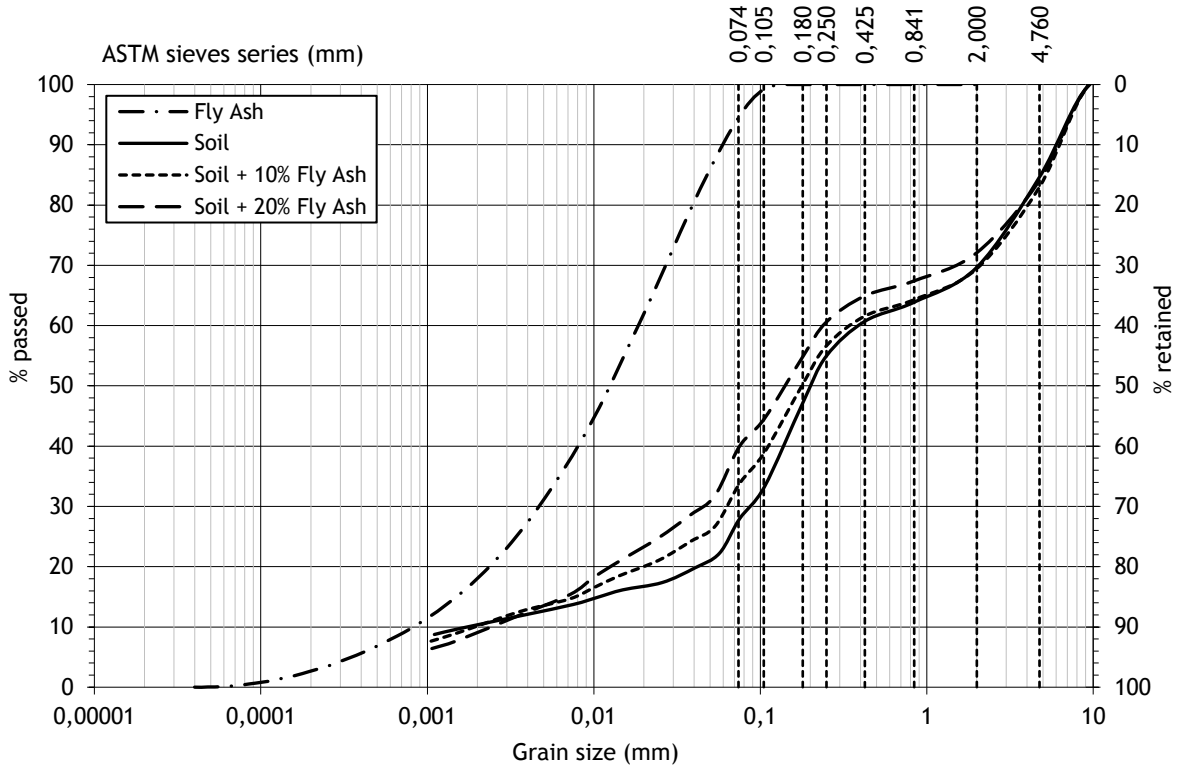

Figure 1. Grain size distribution curve of the soil, fly ash and mixtures

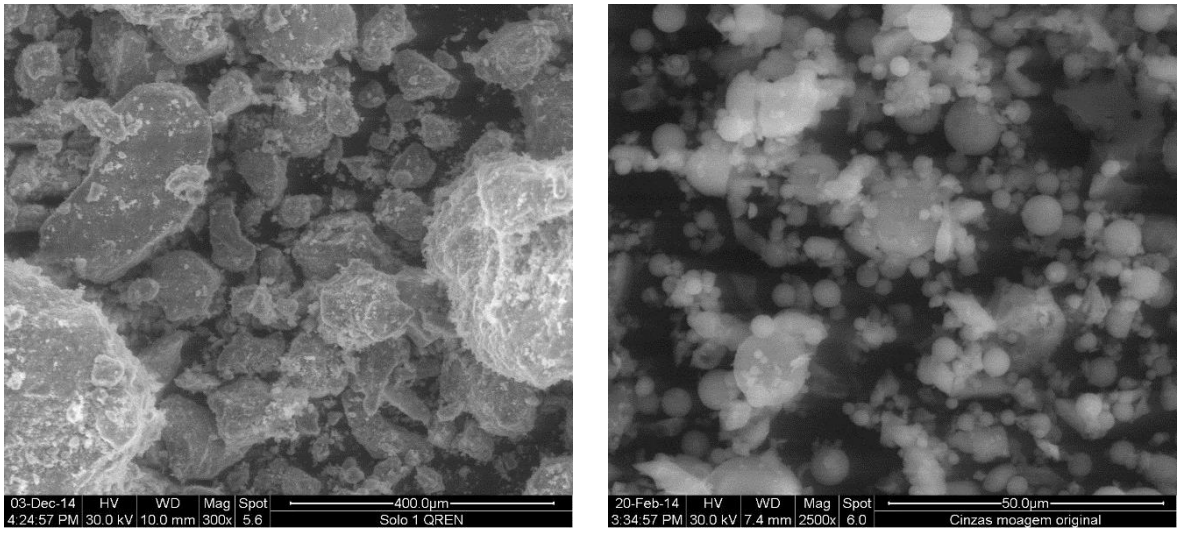

a) b)

Figure 2. SEM micrographs on the particles of soil (a), and fly ash (b),

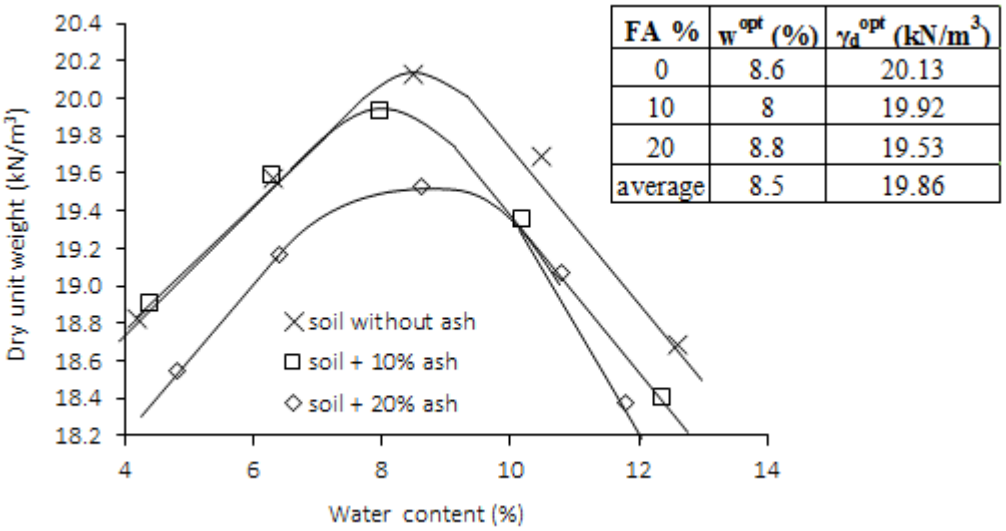

FA %	w^{opt} (%)	γ_d^{opt} (kN/m^3)
0	8.6	20.13
10	8	19.92
20	8.8	19.53
average	8.5	19.86

750

751 Figure 3. Modified Proctor curves of the soil, soil+10% of fly ash and soil+20% of fly ash, and
752 corresponding optimum values
753
754

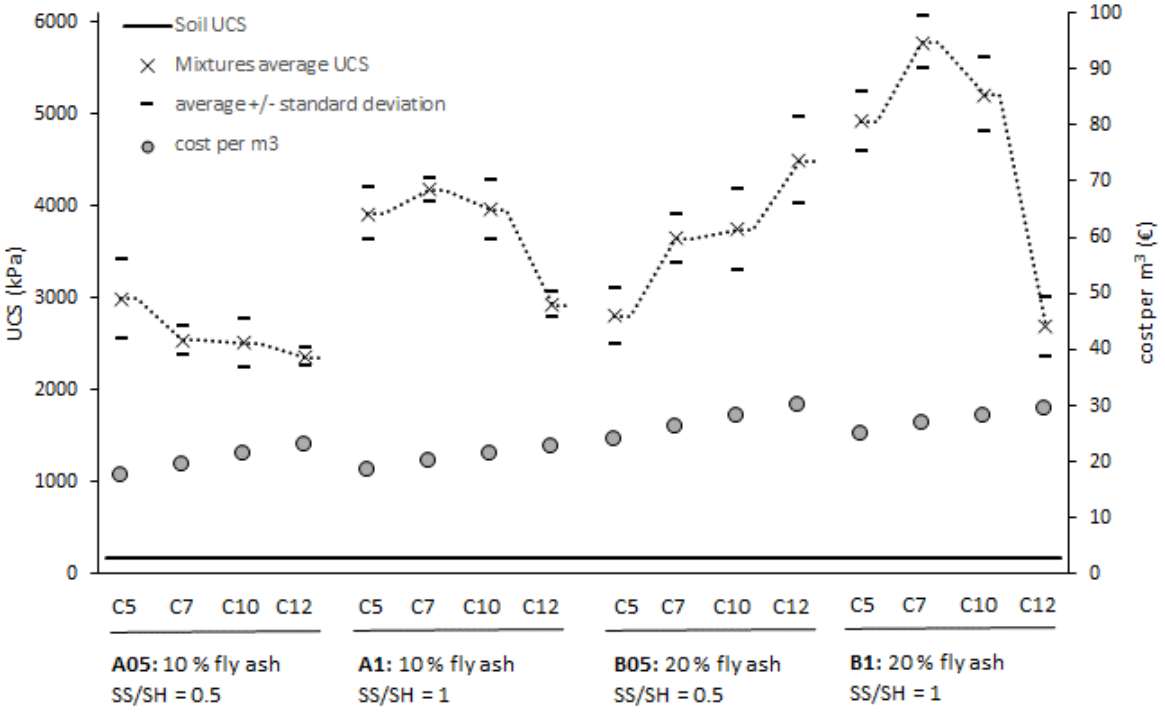

755

756 Figure 4. UCS results at 28 days for the 16 mixtures
757

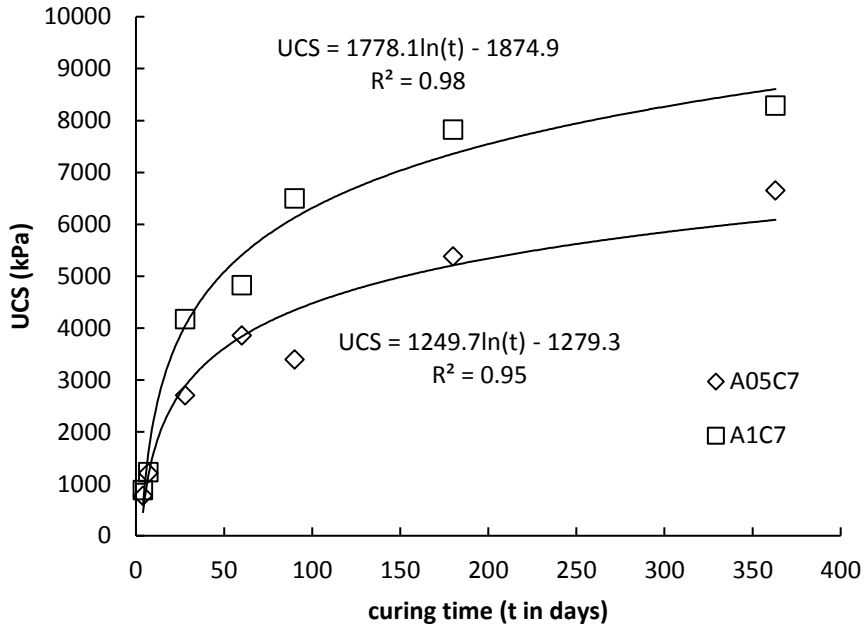

758

759 Figure 5. UCS results up to 360 days for the two selected mixtures
760

761

762

763

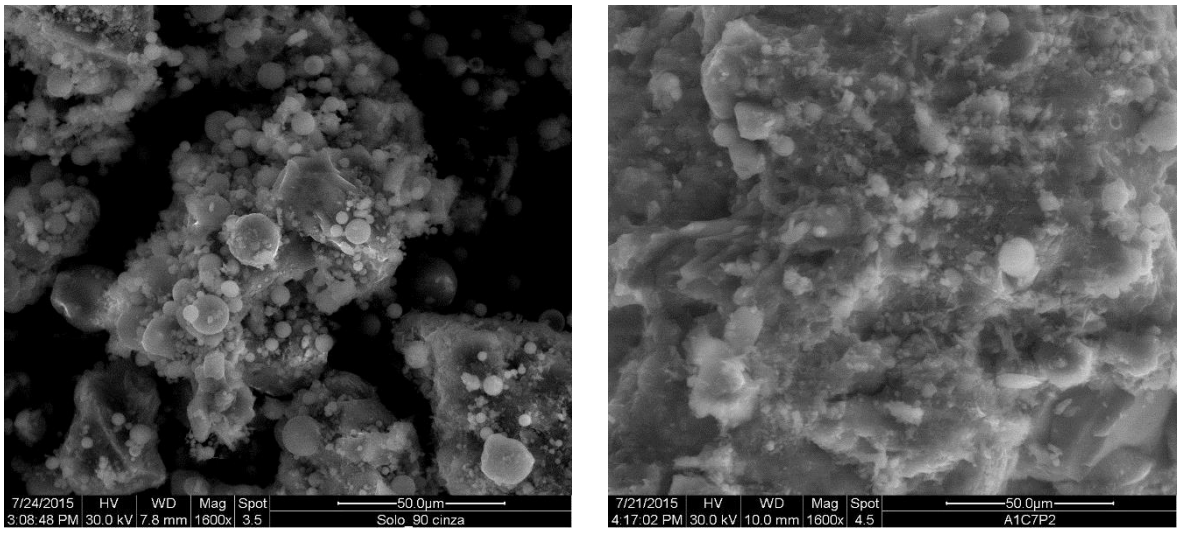

a) b)

764 Figure 6. SEM micrographs of a mixture of soil and fly ash without activator (a), and mixture of soil,
765 fly ash and activator after 1 year of curing period (b)
766

767

768

769

770

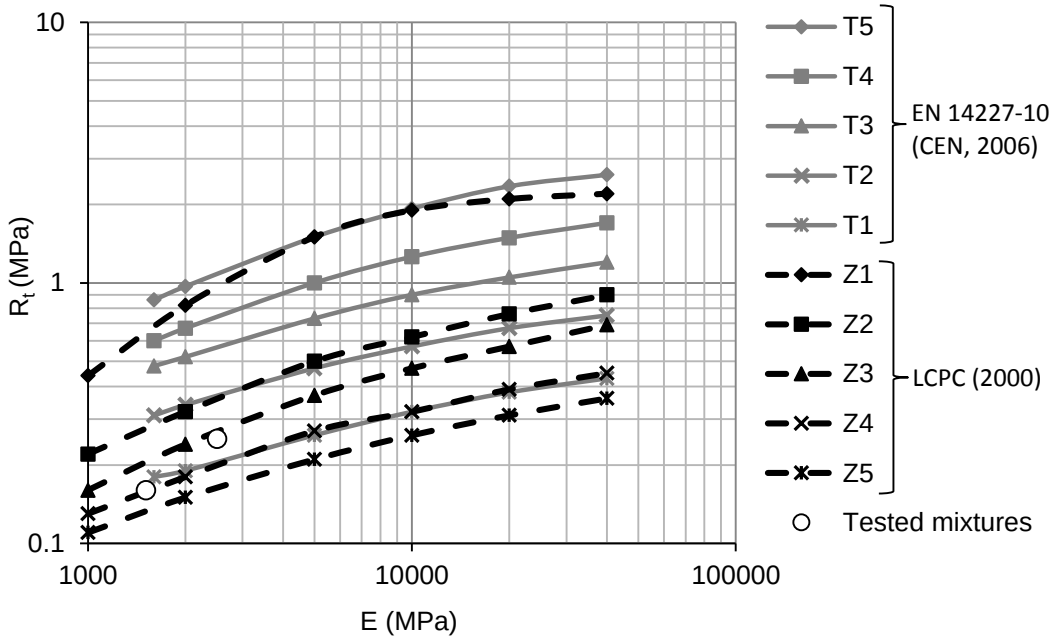

771

772 Figure 7. Material classification zones depending on its stiffness and tensile strength according to EN
773 14227-10 (CEN, 2006) and LCPC (2000)
774

775

776

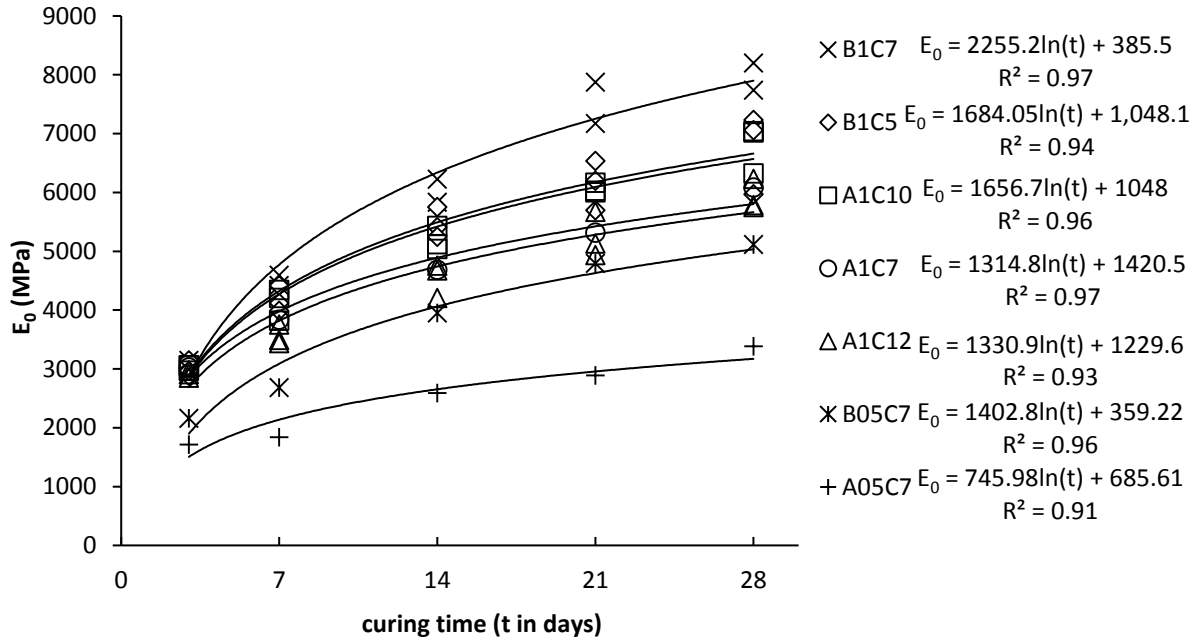

777
778 Figure 8. Young modulus evolution with time for several mixtures
779
780

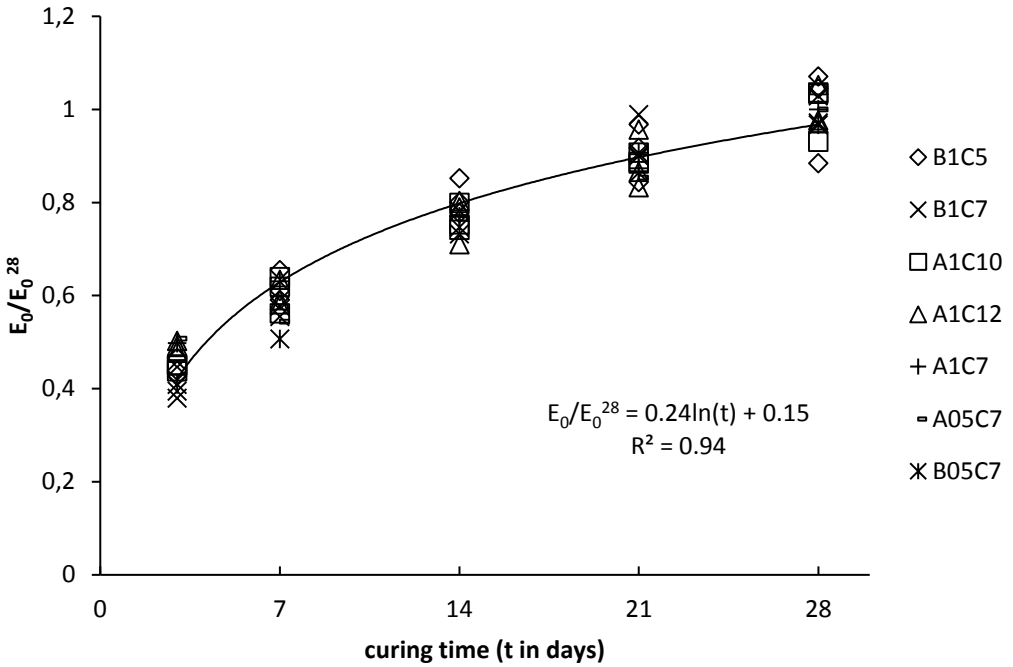

781
782 Figure 9. Normalized Young modulus evolution with time
783

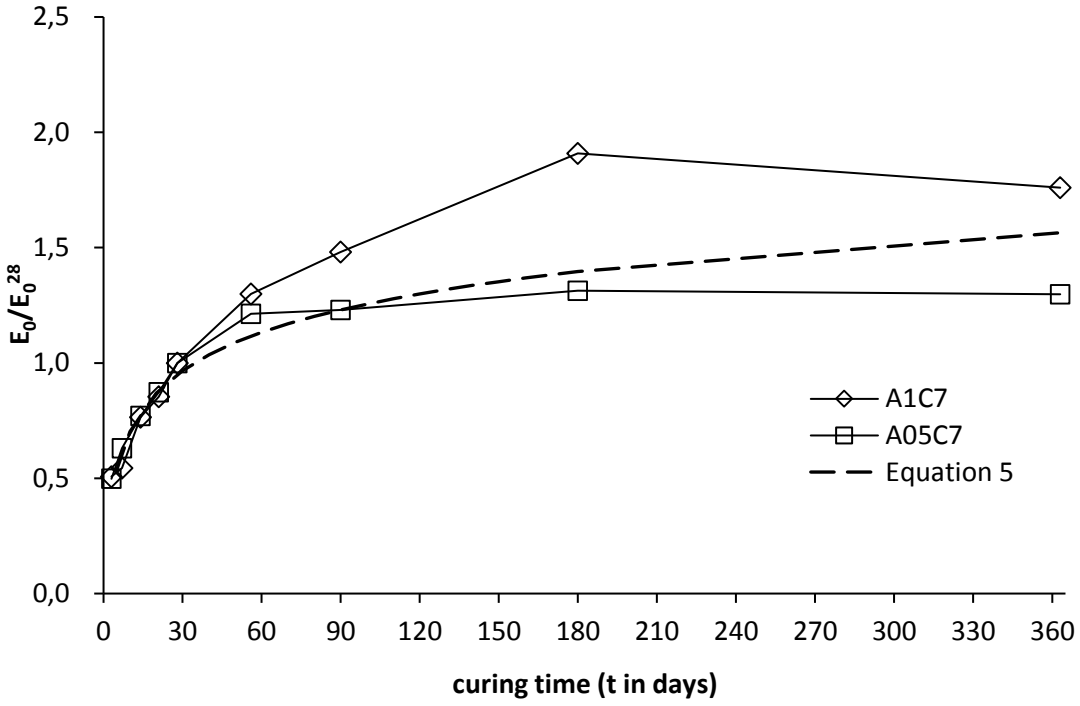

784

785 Figure 10. Young modulus evolution up to 360 days of curing time

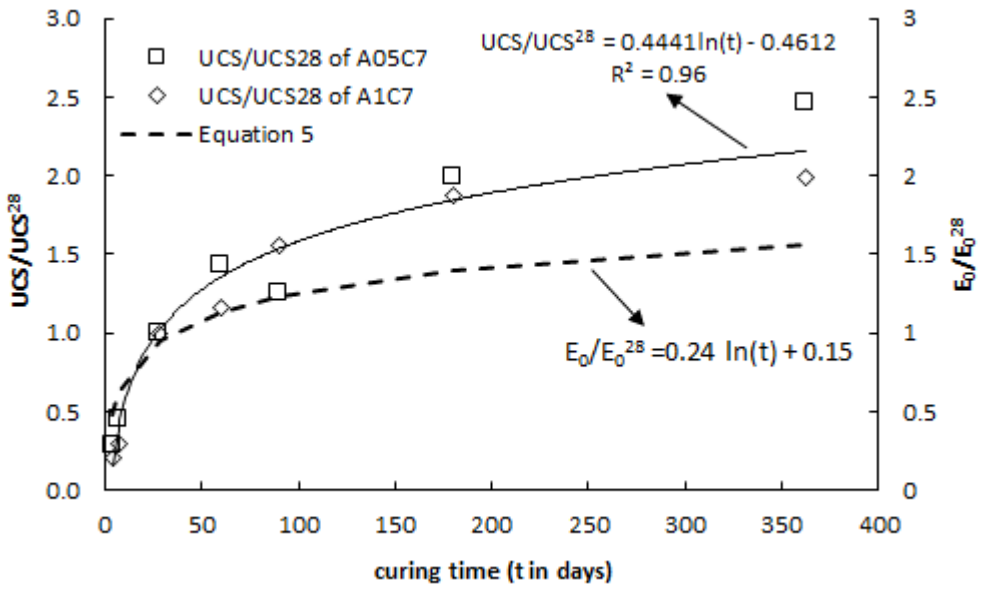

Figure 11. Strength and stiffness evolution with time

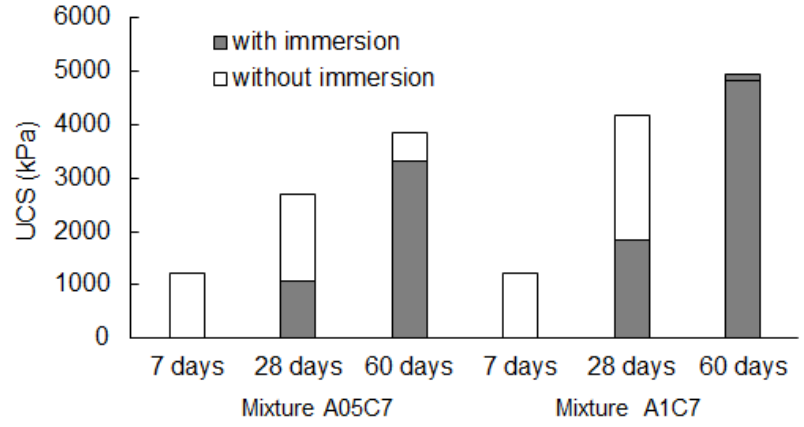

Figure 12. Effect of immersion during curing on the unconfined compression strength of two different mixtures. Note that in the case of specimens tested at 28 days, immersion was performed at 7 days of curing, while for the specimens tested at 60 days, immersion was at 28 days.

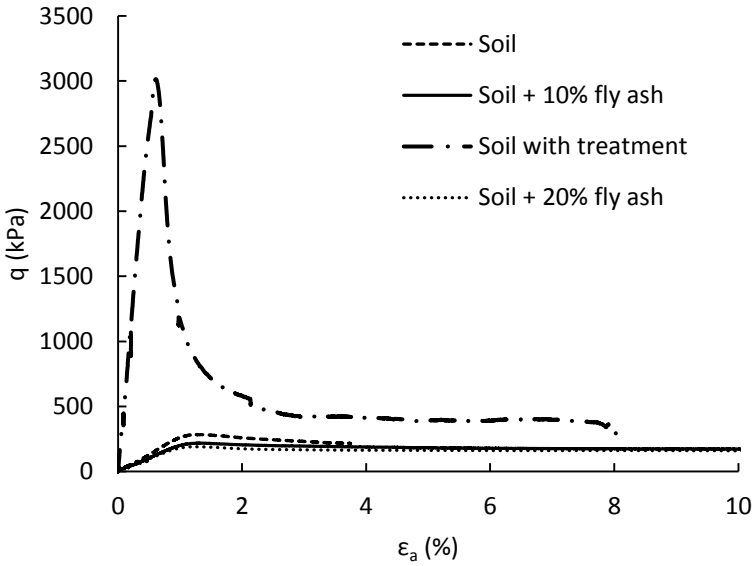

796

797 Figure 13. Stress-strain curves obtained in tested mixtures with and without treatment for 50 kPa of
798 confining pressure
799

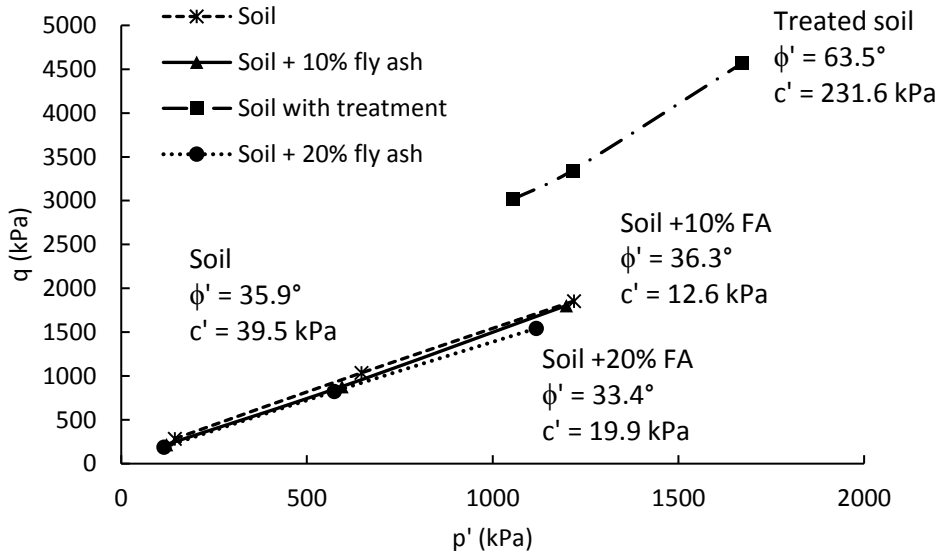

800

801 Figure 14. Strength envelope for the tested mixtures and derived strength parameters
802

803